CT radiomics for predicting PD-L1 expression on tumor cells in gastric cancer

Mengying Xu
Department of Radiology, Nanjing Drum Tower Hospital, The Affiliated Hospital of Nanjing University Medical School

Xiangmei Qiao
Department of Ultrasound, Nanjing Drum Tower Hospital Clinical College of Nanjing Medical University

Song Liu
Department of Radiology, Nanjing Drum Tower Hospital, The Affiliated Hospital of Nanjing University Medical School

Zhengliang Li
State Key Lab of Novel Software Technology, Nanjing University

Changfeng Ji
Department of Radiology, Nanjing Drum Tower Hospital, The Affiliated Hospital of Nanjing University Medical School

Hui Li
Department of Radiology, Nanjing Drum Tower Hospital, The Affiliated Hospital of Nanjing University Medical School

Tingting Shi
Department of Radiology, Nanjing Drum Tower Hospital, The Affiliated Hospital of Nanjing University Medical School

Lin Li
Department of Pathology, Nanjing Drum Tower Hospital, The Affiliated Hospital of Nanjing University Medical School

Qing Gu
State Key Lab of Novel Software Technology, Nanjing University

Kefeng Zhou
Department of Radiology, Nanjing Drum Tower Hospital, The Affiliated Hospital of Nanjing University Medical School

Zhengyang Zhou (zyzhou@nju.edu.cn)
Department of Radiology, Nanjing Drum Tower Hospital, The Affiliated Hospital of Nanjing University Medical School https://orcid.org/0000-0003-2497-8786

Research Article

Keywords: Stomach neoplasm, Programmed cell death ligand 1, Radiomics, Tomography, X-ray computed

Posted Date: November 29th, 2021

DOI: https://doi.org/10.21203/rs.3.rs-52520/v3

Abstract

Purpose To explore CT radiomics for predicting programmed cell death ligand 1 on tumor cells (PD-L1) status in gastric cancer (GC).

Methods From March 2019 to July 2020, 358 patients identified with GC who underwent surgery at our hospital were enrolled in this study retrospectively. All patients were divided into primary (n=239) and validation (n=119) cohorts based on the time of surgery at a ratio of 3:1. Radiomic features were extracted from regions of interest manually drawn on venous CT images. Besides, preoperative tumor markers of all patients were collected and analyzed. The signatures based on radiomics were built using Support Vector Machine (SVM) and Random Forest (RF). Receiver operating characteristic (ROC) curve was performed to assess diagnostic efficiency. Decision curve analysis confirmed the clinical utility.

Results Numerous radiomic features (all p<0.05) differed significantly between GCs with different PD-L1 status. The model developed by SVM algorithm in the primary and validation cohort achieved better performance with AUCs of 0.704 and 0.799, respectively.

Conclusion It was promising to predict PD-L1 status in GCs noninvasively using CT radiomics. It might help to improve clinical decision making with regard to immunotherapy.

Introduction

Gastric cancer (GC) is a common malignancy with the third cause of cancer-associated mortality worldwide [1]. GC is treated in a variety of ways, among which surgery is the preferred treatment. However, for unresectable locally advanced, recurrent, or metastatic GC, palliative management containing systemic treatment is recommended for patients [2].

Immunotherapy has been the focus and hotspot of clinical research since it was proposed. It includes treatments using monoclonal antibodies, cytokines, etc., which are expected to boost host anti-tumor response capability or boost the immunogenicity and sensitivity to treatment of the tumor cells [3, 4]. Recently, the introduction of immunotherapy, particularly the utility of immune checkpoint inhibitors, has improved the prognosis of many cancers [5, 6]. Numerous clinical works demonstrated that programmed cell death protein-1 (PD-1) (a classic immune checkpoint protein) and programmed cell death ligand 1 (PD-L1) are ideal targets for immunotherapy [7, 8]. National Comprehensive Cancer Network guidelines for GC also comprise the treatment of positive PD-L1 expression tumors with monoclonal antibody (Pembrolizumab) [2]. What's more, a recent study indicated that nivolumab (PD-1 inhibitor) in combination with chemotherapy showed superior overall survival along with progression-free survival benefit than chemotherapy alone for advance GCs [9]. Thus, it is crucial to obtain the status of PD-L1.

Currently, the detection of PD-L1 is mainly based on endoscopic biopsy or resected specimens. Endoscopic examination is an invasive procedure with limited samples and possible selection bias, and resected specimens cannot be achieved from unresectable GCs [10]. Hence, a new method is essential to

obtain the status of PD-L1 in GC in a simple, non-invasive, and dynamic manner. In recent years, with the increasingly extensive study of PD-L1 in tumors, medical imaging methods have been used to predict the PD-L1 expression level [11, 12]. Contrast-enhanced computed tomography (CT) is the conventional imaging modality for assessment of GC, which plays a pivotal role in staging and follow-up [2, 13]. Nevertheless, conventional CT images mainly provide simple morphological characteristics instead of complex quantitative parameters.

Radiomics, as an emerging image analysis tool, allows extracting quantitative features noninvasively from digital medical images that enables mineable high-dimensional data to be applied in oncological practice within histological classification, lymph node metastasis, treatment response, and prognosis [14-16]. As previous studies revealed, the presented radiomic-based signatures from CT and the positron emission tomography (PET)/CT were able to achieve significant and robust individualized estimation of specific PD-L1 status in non-small cell lung cancer (NSCLC) and advanced lung adenocarcinoma, respectively [17, 18].

With regard to the evaluation of PD-L1 in GC, it has been reported that GC with positive PD-L1 expression had elevated ^{18}F-fluorodeoxyglucose (^{18}F-FDG) accumulation, and ^{18}F-FDG PET/CT had the capacity to predict the status of PD-L1 [19]. PET/CT has higher radiation and price than CT, which is not a routine examination. To our limited knowledge, no study has been conducted to predict PD-L1 expressions in GC based on CT radiomics. In addition, clinical data, including demographic information and preoperative serum tumor markers, could also be effectively used. Moreover, there is a substantial interest in the use of machine learning algorithms for selecting optimal radiomic features from medical images and applying them to tumor evaluation, as well as in the improvement of diagnostic efficacy [20, 21].

Therefore, we sought to explore the capability of the signatures based on CT radiomics complement clinical data to predict PD-L1 status in GC.

Materials And Methods

Patients

We searched patients who underwent surgery at our hospital between March 2019 and July 2020 consecutively, and 491 patients were identified with GC. The following were inclusion criteria: (1) a pathological confirmation of GC postoperatively and (2) availability of tumor markers and abdominal contrast-enhanced CT within 2 weeks prior to surgery. The following were exclusion criteria: (1) a history of GC treatment before surgery (n=20); (2) insufficient distention of the stomach (n=40); (3) no definite information on PD-L1 (n=12); and (4) poor imaging quality due to respiratory or peristaltic motion (n=16) ; (5) hardly visible on CT images due to the small size of the lesion (n=37); and (6) incomplete information on tumor markers (n=8). The flow chart of patient selection is plotted in Fig. 1. Our Institutional Review Board has approved the current study, following the regulations outlined in the Declaration of Helsinki.

A total of 358 patients (male, 258; female, 100; median age, 60 years; age range, 29-97 years) conformed to the criteria. Patients were divided into primary cohort (n=239) and validation cohort (n=119) at a ratio of 3:1 according to the time of surgery.

CT image acquisition

CT examinations were performed on 64-row scanners (VCT, Discovery HD 750, GE Healthcare, and uCT 780, United Imaging). All patients were requested to fast for at least 6 h and drink 600-1000 mL warm water to distend stomach before examination. All patients were in the supine position, and the scan covered the upper or entire abdomen. The patients were trained to hold their breath during CT scans. Following the unenhanced scan, 1.5 mL/kg iodinated contrast agent (Omnipaque 350 mg I/mL, GE Healthcare) was injected intravenously at a flow rate of 3.0 mL/s using a high-pressure syringe (Medrad Stellant CT Injector System, Medrad Inc.). Imaging was achieved with a post-injection delay of 30-40 s and 70 s after initiation of contrast material injection, corresponding to the arterial and venous phases, respectively. CT scan parameters: tube voltage 100-120 kV, tube current 150-250 mA, slice thickness 5 mm, slice interval 5 mm, field of view 35-50 cm, matrix 512 × 512, rotation time 0.7 s, and pitch 1.0875.

Tumor marker

Six serum tumor markers, including alpha fetoprotein, carcinoembryonic antigen, carbohydrate antigen (CA) 125, CA199, CA724, and CA242, were collected within 2 weeks before surgery.

Image analysis

Axial venous CT images of all patients were downloaded through a picture archiving and communication system and uploaded into Imaging Biomarker Explorer software. A polygonal region of interest (ROI) was manually drawn along the margin of the tumor on maximal transverse slice as illustrated in Fig. 2, carefully avoiding the normal gastric wall tissue and gastric cavity contents. ROI segmentations were performed manually by reader 1 (X.X. with 8 years of experience in abdominal imaging) who was unaware of clinicopathological information of the patients. The general location of the tumors (cardia, body, and antrum) was informed. To evaluate the interobserver reproducibility, 35 cases of CT images were randomly selected for the second ROI segmentation and feature extraction as above by reader 2 (X.X. with 8 years' experience in abdominal imaging). In total, 744 radiomic features were generated automatically from the ROIs. The detailed explanations and formulas of radiomic features are displayed in supplementary material.

Development and performance of signatures

As depicted in Fig. 2, first, the intraclass correlation coefficient (ICC) was calculated to evaluate the interobserver variability of radiomic features extraction using "irr" package (vers. 0.84). Radiomic features with the ICC values >0.8 were regarded as highly reproducible features and initially selected. Second,

the Mann-Whitney U test was used to select significantly different radiomic features between different PD-L1 status groups. The least absolute shrinkage and selection operator (LASSO) was used for the dimension reduction of radiomic features. Then, the optimal variables were put into our in-house software programmed with the R software package (version 3.5.2: http:// www.Rproject.org), and the Support Vector Machine (SVM) and Random Forest (RF) algorithms were applied to generate signatures in the primary cohort. The ratio of the training and testing sets was 4:1. In the training phase, a popular data-preprocessing method in machine learning-Synthetic Minority Oversampling Technique was applied to handle the class imbalance problem. The models were evaluated by repeated stratified (K=5) cross-validation. The models developed was also applied to the validation cohort. In addition, to evaluate the clinical usefulness of the developed model, a decision curve analysis (DCA) was plotted by demonstrating the net benefits graphically for a range of threshold probabilities in the validation cohort.

Detection of PD-L1 Expression Status

The PD-L1 expression status were measured through immunohistochemistry testing for paraffin-embedded tumor tissues in our study. The markers cytokeratin and the lymphocyte common antigen were used to differentiate tumor cells. The positivity for PD-L1 was assessed by one pathologist using SP142 abcam staining. The expression for PD-L1 was scored according to tumor cell / tumor infiltrating lymphocyte proportion, which was defined as the percentage of tumor cells / tumor infiltrating lymphocytes with complete or partial membranous staining at any intensity.

Statistical analysis

The normality distribution of radiomic features was evaluated by the Shapiro-Wilk test. Based on the normality test results, the difference of them was analyzed by the Mann-Whitney U test. Interobserver agreement of radiomic features was estimated with ICC (0.000-0.200: poor; 0.201-0.400: fair; 0.401-0.600: moderate; 0.601-0.800: good; 0.801-1.000: excellent). Receiver operating characteristic (ROC) analysis and the area under the ROC curve (AUC) were performed to evaluate the diagnostic performance of signatures. All those statistical analyses were performed with SPSS (version 22.0 for Microsoft Windows x64, SPSS), MedCalc Statistical Software (version 11.4.2.0 MedCalc Software bvba; http://www.medcalc.org; 2011), and R software package (version 3.5.2: http:// www.Rproject.org). A two-tailed p value <0.05 was considered statistically significant.

Results

Qualitative Data Analysis

The demographic data and pathological information of the included patients are summarized in Table 1.

Quantitative Data Analysis

Tumor marker

There were no significant differences in six tumor markers between GCs with different PD-L1 status in the primary cohort (Table 2).

Radiomic feature

After assessing the reproducibility, the data derived from the tumor ROI on venous CT images were reduced to 665 robust features (interobserver ICC values >0.8) for the subsequent analysis. In addition, there were significant differences in 83 radiomic features derived from venous CT images between negative and positive PD-L1 expressions GCs in the primary cohort. The diagnostic performance of those features ranged from 0.596 to 0.627.

Diagnostic Performance of Signatures

All the significantly different variables were placed into LASSO for dimension reduction (Fig. 3). Ultimately, 10 (F140Percentile, F145PercentileArea, F2135.7Homogeneity, F2315.7Homogeneity, F245.4InverseVariance, F290.4InverseVariance, F2225.4InverseVariance, F2270.4InverseVariance, F4MedianAbsoluteDeviation, F5MedianAbsoluteDeviation) optimal variables were reserved to develop the models using the SVM and RF algorithms in the primary cohort, the model developed by SVM achieved better performance with an AUC of 0.704. The developed model was also applied to the validation cohort with an AUC of 0.799. The DCA for the developed model based on the validation cohort is plotted in Fig 4.

Discussion

PD-1 is a classic immune checkpoint protein, and the utility of PD-1 targeted therapy (depending on the status of PD-L1) is beneficial to improve the prognosis of many cancers [3]. In this current study, we developed and validated the utility of the signatures based on CT radiomics complement clinical data to predict PD-L1 status in GC. Clinical data, including the demographic information and six serum tumor markers, were collected. In addition, 744 radiomic features of GCs based on venous CT images were extracted. Plenty of radiomic features differed significantly between GCs with different PD-L1 status. After the feature selection, 10 robust features were retained, these signatures based on SVM were competent to predict the status of PD-L1 in GCs. However, serum tumor markers and the demographic data, including age and gender, showed no significant differences between negative and positive PD-L1 expressions GCs in the primary cohort.

Nowadays, CT radiomics has been used widely in tumor assessment [14-16], yet only a few of them focused on PD-L1. Our study found that there were abundant radiomic features with statistical significance between GCs with different PD-L1 expressions. All those features were placed into LASSO for dimension reduction, the diagnostic efficiency of SVM increased with AUCs of 0.704 and 0.799 in the primary and validation cohorts, while the AUCs achieved with RF is relatively lower. It indicated that the SVM might be a more suitable algorithm for evaluating the PD-L1 expression in GC. To our limited knowledge, no previous study focused on CT radiomics to predict PD-L1 status of GC, but Chen R, et al. applied SUVmax based on PET to investigate PD-L1 expression in GC with an AUC of 0.822 [19]. Although

the AUC was higher than ours, the sample size was small, and the study lacked validation group for further verification. Besides, for some patients in their study, the specimens for the detection of PDL-1 were obtained only by endoscopic biopsy.

Serum tumor markers, indirectly indicating tumor burden, are commonly used for malignant tumor diagnosis, efficacy evaluation, and prognosis [22-24]. Lang D et al. demonstrated that the early change of serum tumor markers is predictive of progression-free and overall survival in patients with NSCLC treated by PD-1 targeted therapy [25]. In this study, preoperative six tumor markers were also collected and analyzed, though there were no significant differences in tumor markers between GCs with different PD-L1 status in the primary cohort. Depending on our previous literature investigation, no study on the prediction of PD-L1 status in GC by serum tumor markers was found. Therefore, applying tumor markers in the prediction of PD-L1 status in GC needs further exploration.

In this study, we developed and validated radiomic models to assess PD-L1 status in GC preoperatively using relatively large sample size, and it indicated that the models could predict PD-L1 status. Decision curve analysis showed that the radiomic model is useful. Though the serum tumor markers showed no predictive value of PD-L1 status in GC, there insists other clinicopathological information, including hematological parameters and endoscopic biopsy, to be further effectively utilized.

Certain limitations of our study deserve consideration. First, it was a single centre retrospective study with a relatively small sample size. Prospective multicentre studies with large samples need to be carried out to confirm our results further. Second, our feature extraction was restricted to lesions on venous phase, because a prior study suggested [26] that radiomic features derived from venous phase images had superior discrimination of tumor tissue from adjacent normal gastrointestinal wall. Third, ROIs were delineated on the maximal slice images since tumor on that section is the clearest, which might not reflect the overall information of the tumor.

In conclusion, it was promising to predict PD-L1 status in GCs noninvasively using CT radiomics. It might help to improve clinical decision making with regard to immunotherapy.

Data availability

Data are available upon request to the corresponding author.

Reference

1. Bray F, Ferlay J, Soerjomataram I, Siegel RL, Torre LA, Jemal A (2018) Global cancer statistics 2018: GLOBOCAN estimates of incidence and mortality worldwide for 36 cancers in 185 countries. CA Cancer J Clin 68(6):394-424.

2. Ajani JA, D'Amico TA, Almhanna K, Bentrem DJ, Chao J, Das P et al. National Comprehensive Cancer Network. NCCN Clinical Practice Guidelines in Oncology. Gastric Cancer, Version 1.2019. Available at: https://www.nccn.org/professionals/physician_gls/PDF/gastric.pdf. Accessed 14 May 2019.
3. Lazăr DC, Avram MF, Romoșan I, Cornianu M, Tăban S, Goldiș A (2018) Prognostic significance of tumor immune microenvironment and immunotherapy: Novel insights and future perspectives in gastric cancer. World J Gastroenterol 24(32):3583-3616.
4. Niccolai E, Taddei A, Prisco D, Amedei A (2015) Gastric cancer and the epoch of immunotherapy approaches. World J Gastroenterol 21(19):5778-5793.
5. Robert C, Thomas L, Bondarenko I, et al (2011) Ipilimumab plus dacarbazine for previously untreated metastatic melanoma. N Engl J Med 364(26):2517-2526.
6. Bellmunt J, Powles T, Vogelzang NJ (2017) A review on the evolution of PD-1/PD-L1 immunotherapy for bladder cancer: The future is now. Cancer Treat Rev 54:58-67.
7. Philips GK, Atkins M (2015) Therapeutic uses of anti-PD-1 and anti-PD-L1 antibodies. Int Immunol 27(1):39-46.
8. Muro K, Chung HC, Shankaran V, et al (2016) Pembrolizumab for patients with PD-L1-positive advanced gastric cancer (KEYNOTE-012): a multicentre, open-label, phase 1b trial. Lancet Oncol 17(6):717-726.
9. Janjigian YY, Shitara K, Moehler M, et al (2021) First-line nivolumab plus chemotherapy versus chemotherapy alone for advanced gastric, gastro-oesophageal junction, and oesophageal adenocarcinoma (CheckMate 649): a randomised, open-label, phase 3 trial. Lancet 398(10294):27-40.
10. Lee IS, Park YS, Lee JH, et al (2013) Pathologic discordance of differentiation between endoscopic biopsy and postoperative specimen in mucosal gastric adenocarcinomas. Ann Surg Oncol 20(13):4231-4237.
11. Wu T, Zhou F, Soodeen-Lalloo AK, et al (2019) The Association Between Imaging Features of TSCT and the Expression of PD-L1 in Patients With Surgical Resection of Lung Adenocarcinoma. Clin Lung Cancer 20(2):e195-e207.
12. Zhao L, Zhuang Y, Fu K, et al (2020) Usefulness of [18F]fluorodeoxyglucose PET/CT for evaluating the PD-L1 status in nasopharyngeal carcinoma. Eur J Nucl Med Mol Imaging 47(5):1065-1074.
13. Chen CY, Hsu JS, Wu DC, et al (2007) Gastric cancer: preoperative local staging with 3D multi-detector row CT–correlation with surgical and histopathologic results. Radiology 242(2):472-482.
14. Li Q, Qi L, Feng QX, et al (2019) Machine Learning-Based Computational Models Derived From Large-Scale Radiographic-Radiomic Images Can Help Predict Adverse Histopathological Status of Gastric Cancer. Clin Transl Gastroenterol 10(10):e00079.
15. Jin X, Zheng X, Chen D, et al (2019) Prediction of response after chemoradiation for esophageal cancer using a combination of dosimetry and CT radiomics. Eur Radiol 29(11):6080-6088.
16. Ji GW, Zhang YD, Zhang H, et al (2019) Biliary Tract Cancer at CT: A Radiomics-based Model to Predict Lymph Node Metastasis and Survival Outcomes. Radiology 290(1):90-98.

17. Jiang M, Sun D, Guo Y, et al (2020) Assessing PD-L1 Expression Level by Radiomic Features From PET/CT in Nonsmall Cell Lung Cancer Patients: An Initial Result. Acad Radiol 27(2):171-179.
18. Yoon J, Suh YJ, Han K, et al (2020) Utility of CT radiomics for prediction of PD-L1 expression in advanced lung adenocarcinomas. Thorac Cancer 11(4):993-1004.
19. Chen R, Chen Y, Huang G, Liu J (2019) Relationship between PD-L1 expression and 18F-FDG uptake in gastric cancer. Aging (Albany NY) 11(24):12270-12277.
20. Song L, Zhu Z, Mao L, et al (2020) Clinical, Conventional CT and Radiomic Feature-Based Machine Learning Models for Predicting ALK Rearrangement Status in Lung Adenocarcinoma Patients. Front Oncol 10:369.
21. Feng Z, Zhang L, Qi Z, Shen Q, Hu Z, Chen F (2020) Identifying BAP1 Mutations in Clear-Cell Renal Cell Carcinoma by CT Radiomics: Preliminary Findings. Front Oncol 10:279.
22. Feng F, Tian Y, Xu G, et al (2017) Diagnostic and prognostic value of CEA, CA19-9, AFP and CA125 for early gastric cancer. BMC Cancer 17(1):737.
23. Song XH, Liu K, Yang SJ, et al (2020) Prognostic Value of Changes in Preoperative and Postoperative Serum CA19-9 Levels in Gastric Cancer. Front Oncol 10:1432.
24. Shimada H, Noie T, Ohashi M, Oba K, Takahashi Y (2014) Clinical significance of serum tumor markers for gastric cancer: a systematic review of literature by the Task Force of the Japanese Gastric Cancer Association. Gastric Cancer 17(1):26-33.
25. Lang D, Horner A, Brehm E, et al (2019) Early serum tumor marker dynamics predict progression-free and overall survival in single PD-1/PD-L1 inhibitor treated advanced NSCLC-A retrospective cohort study. Lung Cancer 134:59-65.
26. Huang YQ, Liang CH, He L, et al (2016) Development and Validation of a Radiomics Nomogram for Preoperative Prediction of Lymph Node Metastasis in Colorectal Cancer. J Clin Oncol 34(18):2157-2164.

Declarations

Compliance with Ethical Standards

Conflict of interest

The authors of this manuscript declare no relevant conflicts of interest, and no relationships with any companies, whose products or services may be related to the subject matter of the article.

Ethical approval

Institutional review board approval was obtained.

Informed consent

Written informed consent was waived.

Tables

Table 1 Demographic data and histopathological information in the primary and validation cohorts

Characteristics	Primary Cohort		*p*	Validation Cohort		*p*
	PD-L1 Negative (n=197)	PD-L1 Positive (n=42)		PD-L1 Negative (n=97)	PD-L1 Positive (n=22)	
Gender			0.779			0.691
Male	146	32		66	14	
Female	51	10		31	8	
Age (y)			0.522			0.835
≤60	74	18		33	8	
>60	123	24		64	14	
T stage			1.000			0.755
1	6	1		6	1	
2	27	5		12	4	
3	103	23		54	10	
4	61	13		25	7	0.132
N stage			0.165			
0	53	7		28	10	
1-3	144	35		69	12	
Lymphovascular invasion			0.932			0.170
Negative	69	15		46	14	
Positive	128	27		51	8	
Neural invasion			0.069			0.543
Negative	43	4		33	6	
Positive	154	38		64	16	

PD-L1, programmed cell death ligand 1 on tumor cell; *$p<0.05$ with chi-square test or Fisher's exact test (n<5).

Table 2 Statistical description and univariate analysis of tumor markers in the primary cohort

Parameters	PD-L1 Negative	PD-L1 Positive	*p*
AFP (ng/mL)	2.10 (1.35, 3.65)	1.95 (1.45, 3.53)	0.647
CEA (ng/mL)	1.57 (0.73, 3.06)	1.52 (0.72, 5.59)	0.526
CA125 (U/mL)	8.10 (5.70, 11.95)	8.30 (6.40, 9.48)	0.796
CA199 (U/mL)	9.88 (6.32, 24.67)	11.23 (5.96, 49.30)	0.614
CA724 (U/mL)	2.64 (1.20, 4.78)	1.75 (1.14, 7.37)	0.799
CA242 (U/mL)	4.07 (2.59, 10.48)	4.61 (2.78, 13.92)	0.910

The data are presented as median with (1st quartile, 3rd quartile); PD-L1, programmed cell death ligand 1 on tumor cell; AFP, alpha fetoprotein; CEA, carcinoembryonic antigen; CA, carbohydrate antigen; *$p<0.05$ with Mann-Whitney U test.

Figures

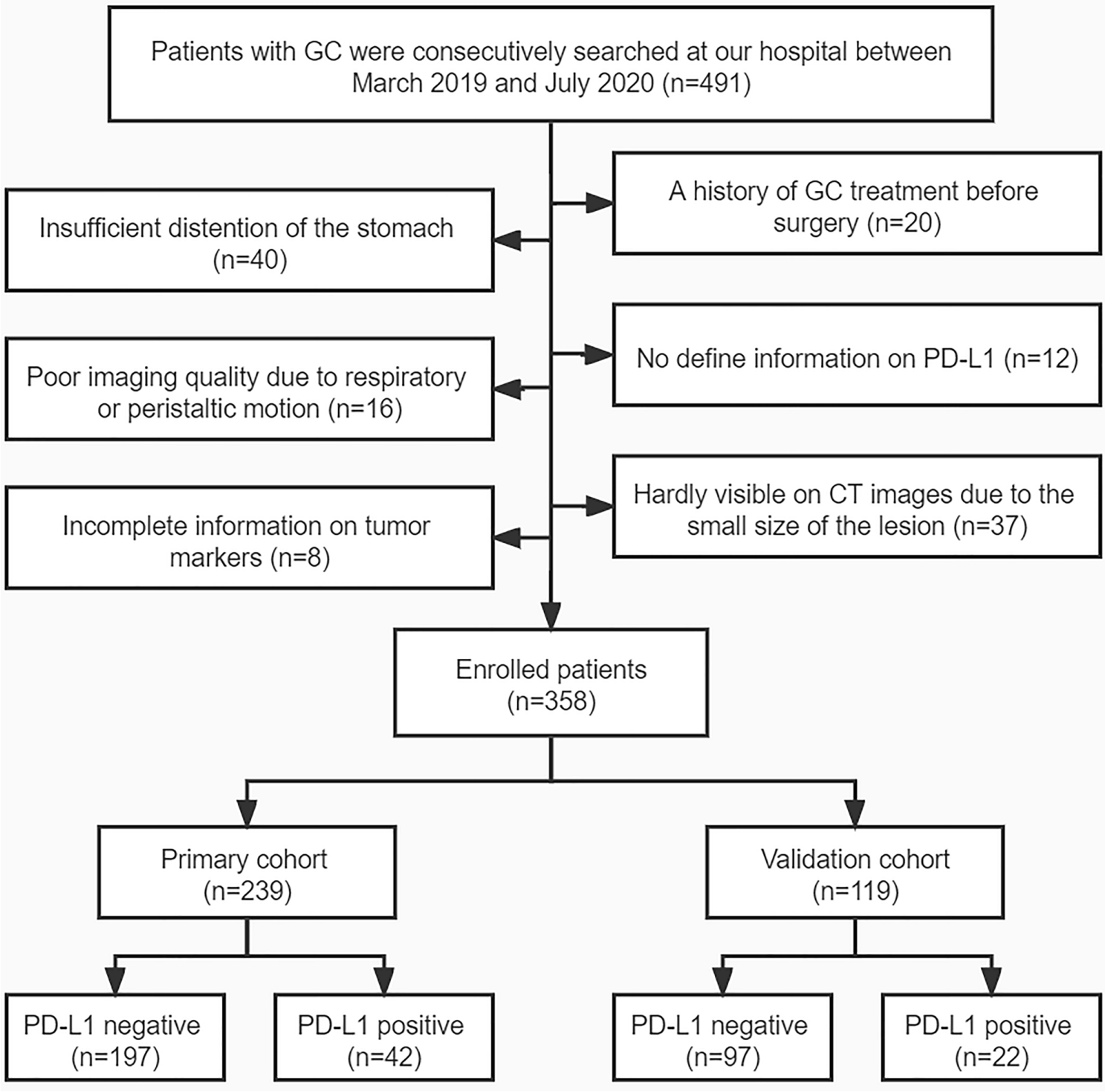

Figure 1

The flow chart of the enrolled patients in our study. GC, gastric cancer; CT, computed tomography; PD-L1, programmed cell death ligand 1 on tumor cell.

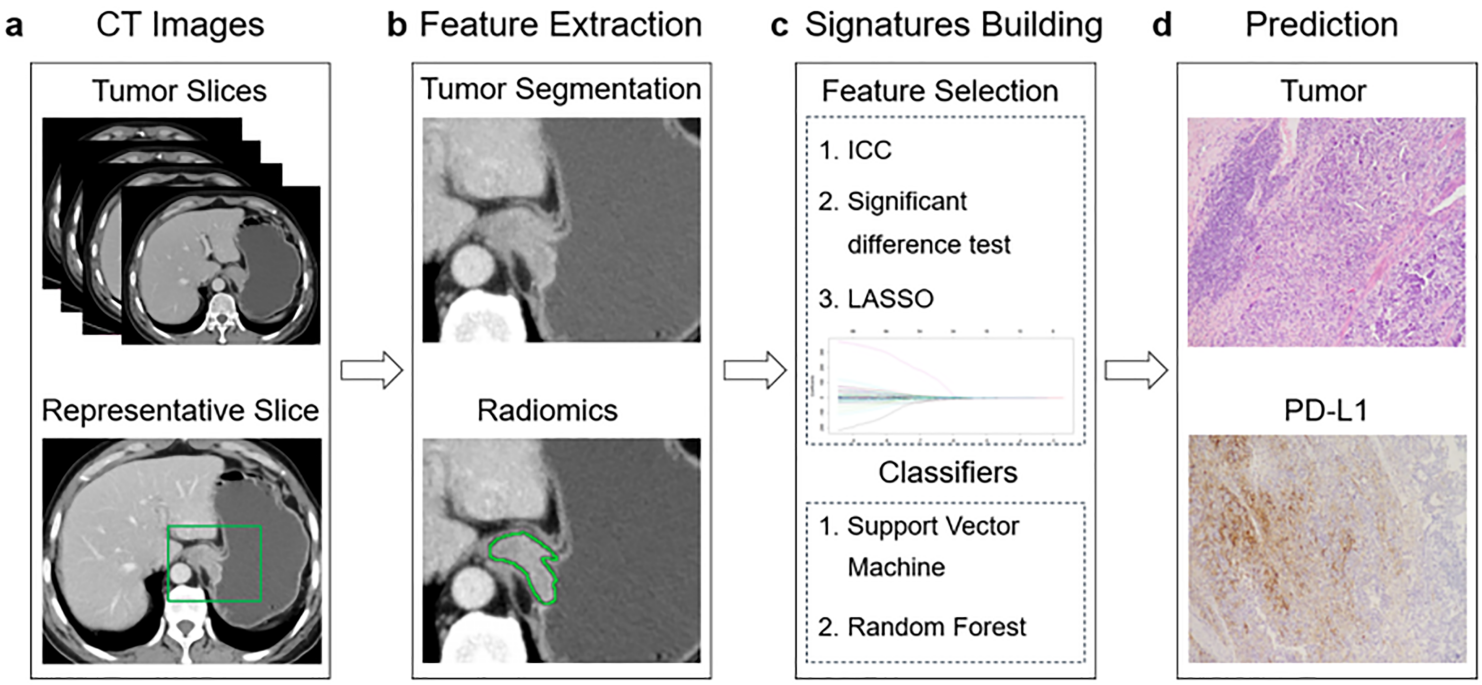

Figure 2

The workflow of this study. On venous CT images, (a) the representative slices of the tumor were selected to extract radiomic features. (b) An ROI was delineated manually along the border of the tumor. (c) ICC, significant difference test, and LASSO were used to screen optimal radiomic features. Signatures based on classifiers were constructed using selected radiomic features. (D) To predict PD-L1 expressions in gastric cancer. CT, computed tomography. ROI, region of interest; ICC, intraclass correlation coefficient; LASSO, least absolute shrinkage and selection operator; PD-L1, programmed cell death ligand 1 on tumor cells.

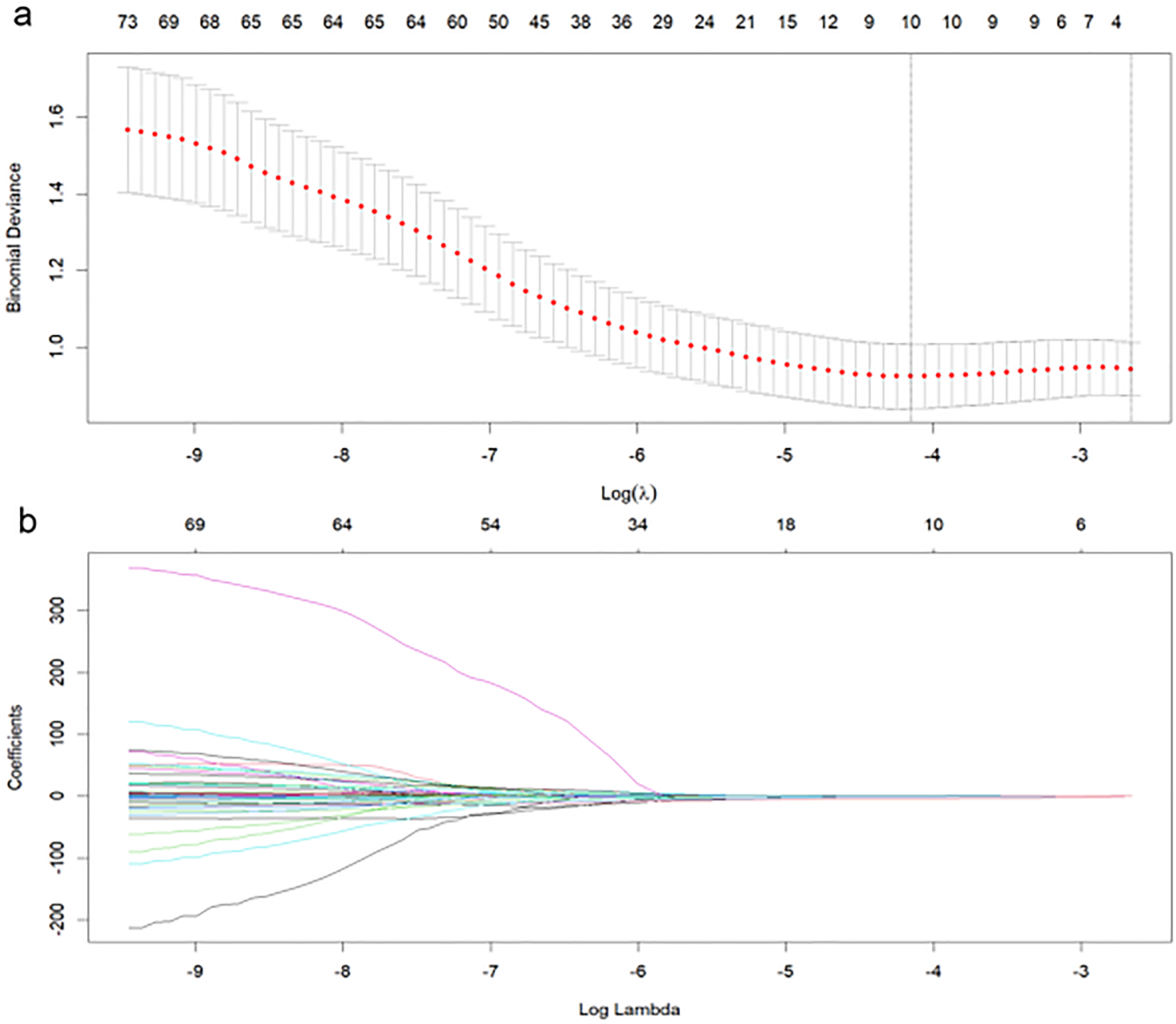

Figure 3

Feature selection was performed using the least absolute shrinkage and selection operator (LASSO) regression model. (a) Tuning parameter (λ) selection in the LASSO model used fivefold cross-validation via minimum criteria. Vertical lines were drawn at the optimal values using the minimum criteria and 1 standard error of the minimum criteria. The optimal λ value of 0.0158 with log (λ)=−4.1480 was chosen. (b) LASSO coefficient profiles of the 83 selected features. A coefficient profile plot was generated versus the selected log (λ) value using fivefold cross-validation; ten selected features with nonzero coefficients were retained.

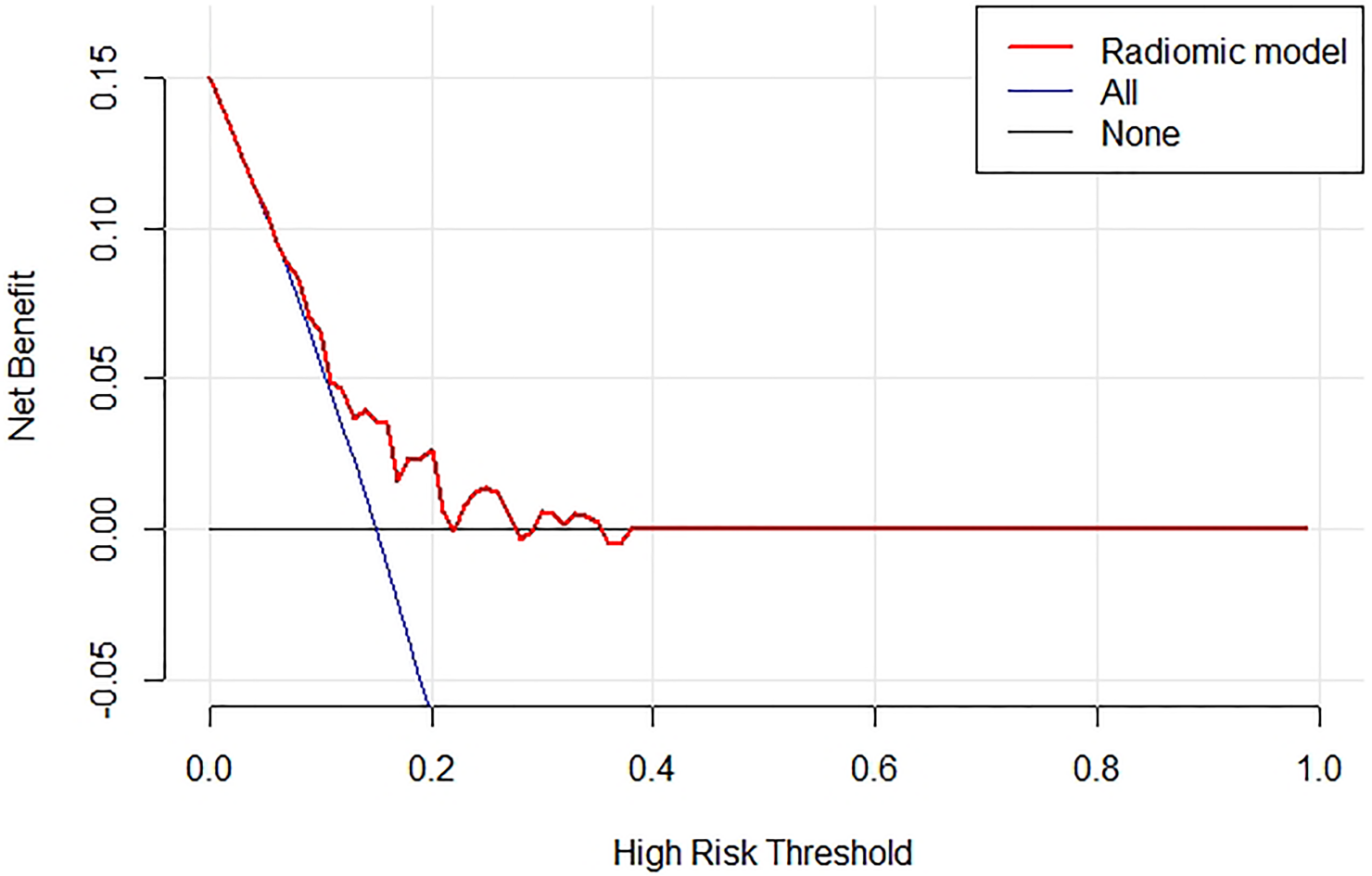

Figure 4

Decision curve analysis for the radiomic model in the validation cohort. The y-axis indicates the net benefit; x-axis indicates threshold probability. The radiomic model (red line) had the highest net benefit compared with the simple diagnoses such as all PD-L1 positive GC patients (blue line) or all PD-L1 negative GC patients (black line) across the majority of the range of reasonable threshold probabilities at which a patient would be diagnosed as PD-L1 positive.

Supplementary Files

This is a list of supplementary files associated with this preprint. Click to download.

- SupplementaryMaterial.docx